



## OPEN ACCESS

## EDITED BY

Cicheng Zhang,  
Hunan Normal University, China

## REVIEWED BY

Siya Shao,  
Berkeley Lab (DOE), United States  
Meng Wang,  
Northeast Normal University, China

## \*CORRESPONDENCE

Xiaoge Wang,  
✉ 17391826018@163.com

RECEIVED 06 June 2025

REVISED 15 September 2025

ACCEPTED 22 September 2025

PUBLISHED 22 January 2026

## CITATION

Wang X, Xue W, Ruan Y, Cheng M and Ma S (2026) Estimation of carbon storage and influencing factors for urban green spaces: a view of green space types and plant community structure. *Front. Environ. Sci.* 13:1642030. doi: 10.3389/fenvs.2025.1642030

## COPYRIGHT

© 2026 Wang, Xue, Ruan, Cheng and Ma. This is an open-access article distributed under the terms of the [Creative Commons Attribution License \(CC BY\)](https://creativecommons.org/licenses/by/4.0/). The use, distribution or reproduction in other forums is permitted, provided the original author(s) and the copyright owner(s) are credited and that the original publication in this journal is cited, in accordance with accepted academic practice. No use, distribution or reproduction is permitted which does not comply with these terms.

# Estimation of carbon storage and influencing factors for urban green spaces: a view of green space types and plant community structure

Xiaoge Wang<sup>1\*</sup>, Wei Xue<sup>2</sup>, Yu Ruan<sup>1</sup>, Mengyao Cheng<sup>3</sup> and Shuying Ma<sup>3</sup>

<sup>1</sup>Assistant Professor, Faculty of Ecological and Environmental Engineering, Yangling Vocational & Technology College, Yangling, Shaanxi, China, <sup>2</sup>Assistant Professor, College of Soil and Water Conservation Science and Engineering, Northwest A&F University, Yangling, Shaanxi, China, <sup>3</sup>College of Horticulture, Northwest A&F University, Yangling, Shaanxi, China

Urban green space (GS) is a major spatial carrier for carrying out carbon sequestration (CS) function. The CS capacity of GS is affected by different resource circumstances, climatic traits, and urban management policies. By examining the variations in carbon storage and the affecting variables across many kinds of GSs and suggesting optimization plans, urban planners may scientifically boost the CS of GS. Focusing on the Xi'an urban region, in this paper, we estimate and examine the carbon storage and spatial distribution features of various kinds of GSs in the Xi'an urban area using field survey and remote-sensing technology. The findings reveal notable changes in the carbon storage capacity of multiple kinds of GSs as well as varying influences of their landscape design elements on carbon storage. By choosing representative plant communities in Xi'an World Expo Park, in this paper, we investigate the link between CS effect and plant community structure. The findings of the study indicate that the tree diameter at breast height and plant community density positively correlate with the carbon storage per unit area; regression analysis reveals the pattern of curve changes in plant community CS impact. A sustainable CS point of view optimization plan for urban GS CS has been suggested based on the above findings.

## KEYWORDS

urban green space, carbon storage, spatial pattern, plant community, carbon sequestration capacity

## 1 Introduction

The continuous increase in the atmospheric CO<sub>2</sub> level has caused global temperatures to increase dramatically, and carbon cycling has been a main focus of research on global climate change (Jiang, 2021; Hausfather et al., 2022). Cities, which are a key component, choose solutions to fight climate change (Wang et al., 2022). As the main spatial carriers of human activity, cities are responsible for 80% of the global energy and carbon emissions. The urban population is expected to be 70% of the world's total population by 2050; the urbanization process will undoubtedly have a major impact on global carbon cycling and climate change. Therefore, all strategies that are intended to fight climate change depend on

cities. Urban green space (GS) is the area where cities may directly act as a carbon sink; a carbon sink is the main research focus of the urban ecosystem carbon cycle (Nowak and Crane, 2002; Wang and Shi, 2015). Plants draw CO<sub>2</sub> from the air using photosynthesis, thereby fixing carbon components and balancing the CO<sub>2</sub> level in the surroundings. Consequently, the carbon sequestration (CS) function of urban GSs has gained attention and developed into a new research hotspot (Shi et al., 2023; Wei et al., 2021; Seto et al., 2012; Zhang et al., 2014; Wang, 2009; Zhu, 2020).

GSs within cities have been shown to capture a lot of carbon in several studies (Seto et al., 2012; Zhang et al., 2014; Wang et al., 2022; Zhao et al., 2013; Nowak et al., 2013); therefore, they are an excellent strategy to offset CO<sub>2</sub> emissions. Although plant carbon storage in urban areas in the United States accounts for 3.2% of the national forest carbon sink, studies have revealed that the carbon absorption capacity of conventional urban GSs in Europe and China can absorb or offset up to approximately 7% of the yearly carbon emissions of the city (Zhao et al., 2013; Nowak et al., 2013). Hangzhou's wood carbon sink can offset 18.57% of industrial carbon emissions annually (Liu and Li, 2012). The results of the research show a good correlation among the green covering rate, GS area, and GS carbon storage. The landscape design strategy of urban GSs makes them more scientific in terms of GS distribution, community organization, and urban administration, thus having some CS potential.

Research has shown significant differences in the CS capacity across many kinds of GSs such that the tree species composition and the vegetation structure are key components characterizing carbon storage. Research has shown that the carbon storage of urban forests is much larger than that of park GSs, street GSs, and grass GSs (Nowak et al., 2013). This is mainly because trees dominate urban forest vegetation, with rich plant layers and high biomass.

Park GSs provide greater average carbon storage than street GSs and residential GSs because the plant types of street GSs and residential GSs are single, and the quantity of trees is limited (Davies et al., 2011; Nowak et al., 2013). However, tree-ruled GSs have a higher carbon fixation capacity, mainly because of their larger biomass, better photosynthesis, and longer carbon storage duration (Nowak et al., 2013); shrubs and grass GSs have reduced carbon fixation capacity because of their smaller biomass, lack of structural carbon pools, and constant cutting (Velasco et al., 2016).

The structural properties of plant communities have a major effect on their carbon storage capacity. Research has shown that the diameter at breast height (DBH) has a major impact on carbon storage. Tree species with a larger DBH, such as those with an average DBH >30 cm, provide far more carbon storage than young trees with DBH <10 cm (Wang et al., 2021).

The impact of community density on the CS capacity is twofold: the planting density affects the light intensity that plants in the plant community receive, where the greater plant density in urban GSs raises their CS capacity, and conversely, competition lowers photosynthesis; thus, low-density communities have more carbon fixation efficiency per plant (Velasco et al., 2016; Nowak and Crane, 2002; Wang et al., 2021). Moreover, changes in the plant structure affect microclimates and habitats, including light, wind, temperature, and humidity, which could also affect the carbon storage function of the community.

A scientific evaluation of the CS capacity of urban GS systems could help to create more exact and feasible emission reduction targets. At present, research on carbon evaluation of urban GS systems mostly focuses on particular types, including park GSs, auxiliary GSs, and street GSs (Wang et al., 2021; Chen et al., 2024; Davies et al., 2011; Velasco et al., 2016). The 2017 Chinese Urban GS Classification Standard (GB/T 51346–2017) clarifies the category system of urban GSs, thus scientifically increasing the degree of urban GS planning and construction.

Variations in vegetation kinds, planting density, community structure, and habitat types in urban GSs cause plants' CS function to differ. Therefore, in cities with high land-use efficiency and progressively limited GS development, there is an increasing demand for concentrated knowledge of the effect of the internal characteristics of urban GS systems on carbon storage in urban GSs, such as GS types, community structures, and landscape patterns.

This paper, therefore, looks at the following questions: different types of GSs in Xi'an support GS carbon storage and spatial patterns using the gauge link between urban GS's carbon storage capacity and its inherent qualities. In terms of sustainable carbon sequestration, the current study is directed toward CS strategies for different types of urban GS.

## 2 Methods and materials

### 2.1 Overview of the research area

Xi'an is located in the central part of the Guanzhong Plain between the 107° 40' and 109° 49' E longitudes and 33° 39' and 34° 45' N latitudes. It is characterized by the moderate temperate semi-humid continental monsoon environment with hot and humid summers and cold and dry winters. The annual average temperature is 13.3 °C; the annual average rainfall, which is largely concentrated from July to September, is 613.7 mm.

The urban area consists of Lianhu District, Beilin District, Yanta District, Baqiao District, Weiyang District, and Xincheng District. The area has various unique plant species ranging from more than 233 species in 183 genera spread throughout 79 groups. In 2022, Xi'an city spanned 807.57 square kilometers, with a green covering rating of 41.85%. Focusing on the metropolitan area of Xi'an city in 2020, this study covers approximately 600 square kilometers.

### 2.2 Processing and data sources for remote sensing

Using the normalized vegetation index (NDVI) and vegetation cover statistics derived from satellite remote-sensing data, in this paper, we map the expansion of urban GS vegetation in Xi'an. Studies indicate that the NDVI in the Shaanxi area is rather high in July and August. Thus, for the computation of the NDVI and vegetation coverage data, in this work, we choose satellite remote-sensing images from Xi'an with low cloud cover from July to August.

This research utilizes the Gaofen-1 satellite remote-sensing picture of Xi'an on 6 July 2020, which was sourced from the Geospatial Data Cloud website (<http://www.gscloud.cn/>). The downloaded photos, at a 30 m × 30 m resolution, show under

TABLE 1 Area proportion (%) of different green space types.

Green space types	Accessory green space (AG)	Protective green space (PG)	Garden green space (GG)	Plaza green space (SG)	Regional green space (RG)
Green space area (%)	7.72	15.25	3.87	0.07	73

TABLE 2 Landscape pattern index.

Landscape pattern	Landscape indices	Level	Ecological significance
Landscape composition	Patch area (CA)	Type	The area of urban green space landscapes
	Patch density (PD)	Landscape/type	The landscape density of urban green space areas
	Numbers of patch (NP)	Landscape/type	The quantity of a specific type of patches
	Largest patch index (LPI)	Landscape	The proportion of the area occupied by the largest patch within the landscape
	Percent of landscape (PLAND)	Type	The proportion of a specific landscape type within the entire landscape
Landscape on figuration	Perimeter area fractal dimension (FRAC)	Type	Assess the complexity of patch boundaries and the degree of landscape fragmentation
	Aggregation index (AI)	Type	The degree of aggregation of green spaces
	Landscape division index (DIVISION)	Landscape/type	The degree of landscape fragmentation and isolation

5% cloud cover across the study region. ENVI was used for remote-sensing picture preprocessing, including geometry correction, radiometric, and atmospheric adjustment. The aboveground carbon storage in cities will subsequently be calculated using the NDVI.

## 2.3 Research framework and methods

### 2.3.1 Classification of urban GS

GS data were gathered in this paper from the urban area of Xi'an city using the CART decision tree classification method. Finally, two land feature types were discovered: GS and non-GS. The spectral properties, texture features, form features, and other unique qualities were selected to classify all types of samples and to obtain GS data (Zhao et al., 2021).

Based on the functions, layout, planting techniques, and management characteristics of GS in urban land combined with China's "Classification Standards for Urban GS (CJJ/T85-2017)" and the actual condition of the study area (standard reference), GSs in the study area are classified into park GSs, protective GSs, square GSs, ancillary GSs, and regional GSs. Table 1 reveals many GSs in the Xi'an metropolitan region in 2020.

### 2.3.2 Landscape pattern index

Depending on the physical environment conditions and the land-use characteristics of Xi'an city, two levels—the landscape level and type level—were selected for a total of eight landscape pattern indices. Among them, patch area (CA), patch number (ND), patch density (PD), maximum patch index (LPI), and landscape category ratio (PLAND) characterize the quantity and relative frequency of landscape components or landscape characteristics.

Reflecting the characteristics of landscape configuration, landscape segmentation index (DIVISION), border complexity (FRAC), and landscape aggregation degree (AI) might provide information regarding landscape shape and spatial organization. Batch generating the specific values of each grid in Fragstats 4.2, utilizing a grid analysis approach, was based on preprocessed land-use data. Table 2 shows the specific relevance of the landscape pattern index.

### 2.3.3 Estimation of carbon storage in urban GSs

Based on the NDVI as a quantitative measure of urban GS carbon sink, this research estimated the aboveground carbon (AGC) of urban GS using remote sensing. Findings from earlier studies (Yao et al., 2015) might help one to infer the link between the NDVI and urban aboveground carbon storage.

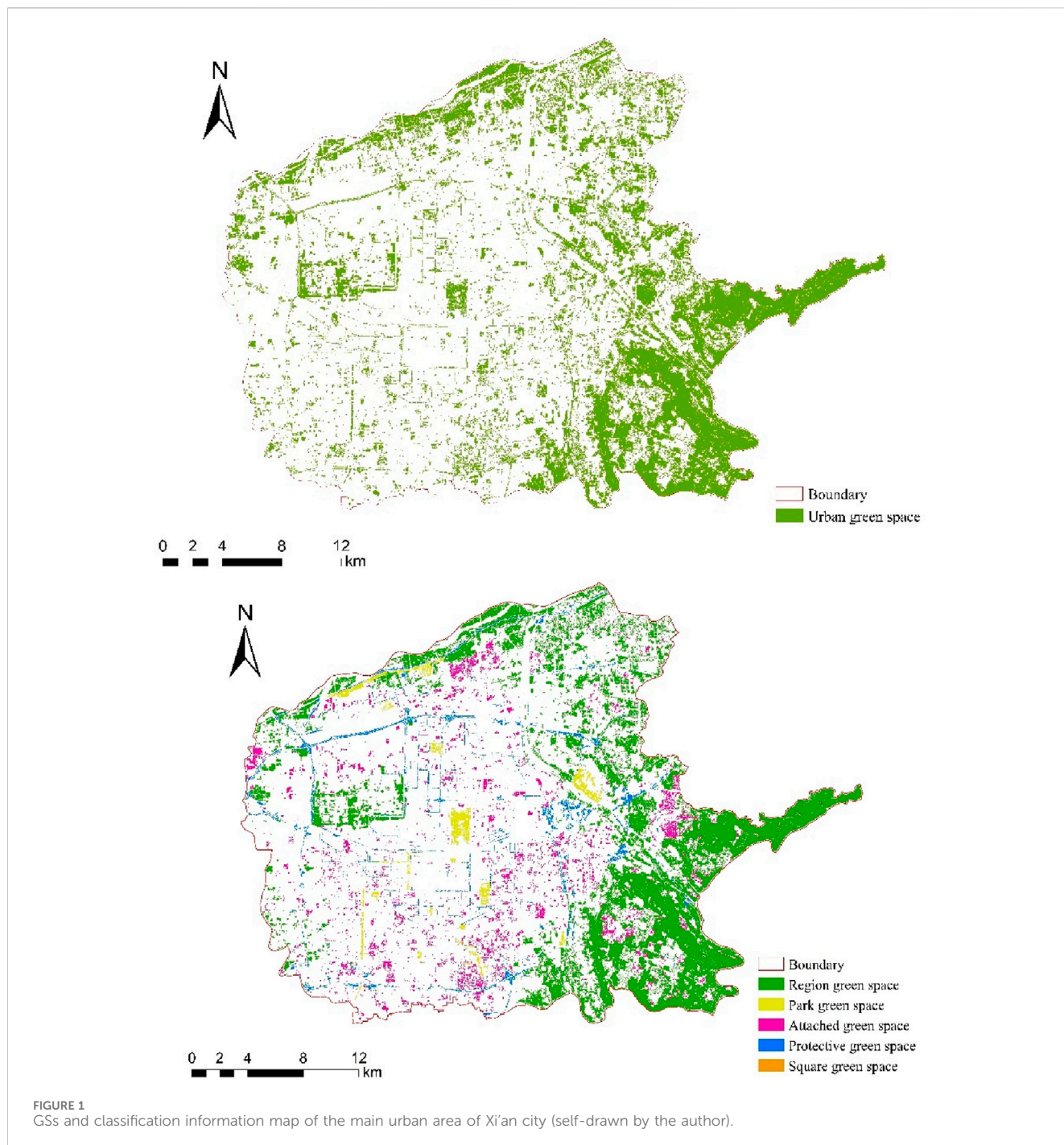
$$YAGC = 6445.014 \times NDVI \times 2.39. \quad (1)$$

In the formula, the YAGC refers to Equation 1 indicates aboveground carbon storage per unit area, which is measured in kg C/pixel; the NDVI is the normalized vegetation index value obtained from the corresponding remote-sensing band operation.

### 2.3.4 Calculation of carbon storage in plant communities

#### 2.3.4.1 Site selection

Figure 1 illustrates the GSs and classification information map of the main urban area of Xi'an city. Covering over 418 ha, the Xi'an World Expo Park is located on the east bank of the Bahe River and hosted the 2011 Xi'an International Horticultural Expo. In the Chanba District, it represents a significant urban biological environment and an important component of urban GSs. Having



moderate continental climate, it averages a yearly temperature of 11.3 °C–13.7 °C. Covering 188 ha, the park is rich in water resources.

Built over more than 10 years, the World Expo Park is equipped with well-developed infrastructure and a consistent environment. With more than 200 types of herbaceous plants, shrubs, and trees planted, the park has sufficient vegetative resources. Forty plant communities, each spanning approximately 400 square meters, revealed various spatial patterns that were randomly chosen in the research area (Figure 2).

Mainly made up of trees and shrubs, the community composition of the research plots showed consistent growth

spread throughout terrestrial regions. Using a DBH tape, laser measuring device, tape measure, canopy analyzer (LAI-2000), and portable photosynthesis analyzer (CIRAS-3), we assessed the community structure attribute factors, namely, the crown width, plant height, breast height diameter, leaf area index, and photosynthetic rate.

For the study, we choose strong plants that were unobstructed by other buildings, had minimum pruning, and were located in clear, windless, and naturally bright environments. From each vigorously growing and comparable plant on the sunny side, five mature leaves were chosen. The leaves were pressed within the leaf chamber for

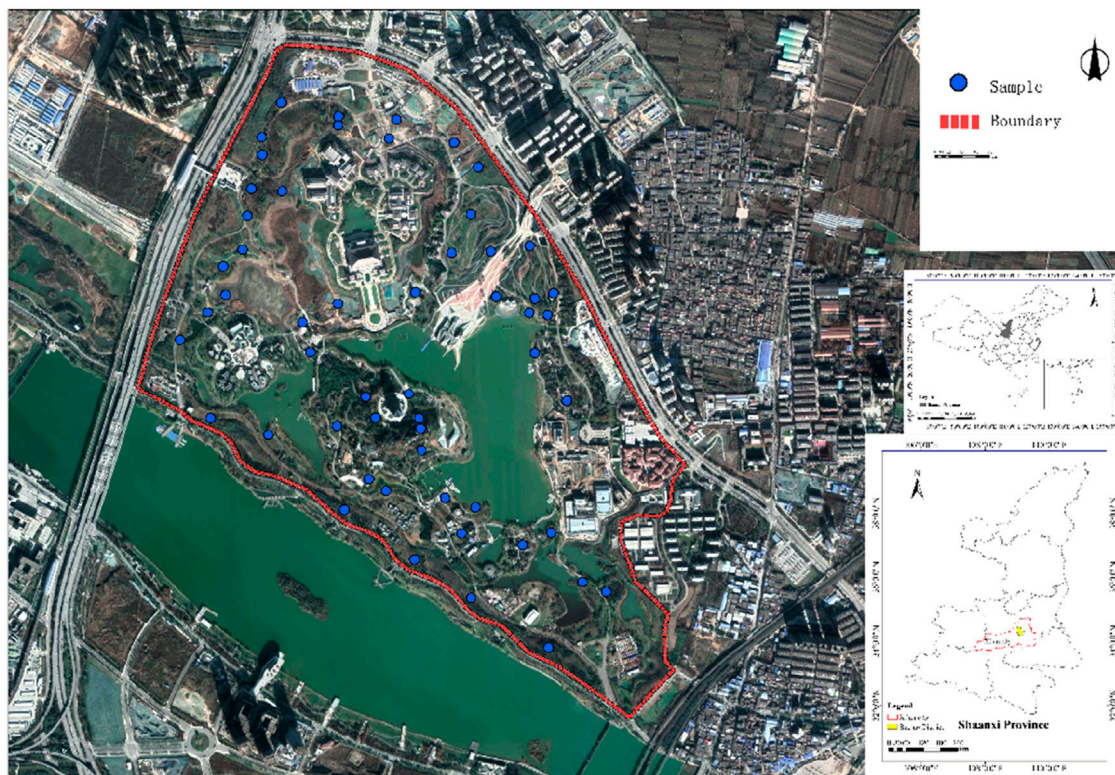


FIGURE 2 Study on the location analysis and community plot distribution map.

TABLE 3 Formula for calculating the DCS per plant.

Number	Formula	Specification
1	$p = [(p_{i+1} + P_i)/2 \times (t_{i+1} - t_i) \times 3,600/1,000$	$p$ is daily assimilation per unit leaf area ( $\text{mmol}\cdot\text{m}^{-2}$ ) $P_i$ is the instantaneous photosynthetic rate of the initial measurement point ( $\text{umol}\cdot\text{m}^{-2}\cdot\text{s}^{-1}$ ) $p_{i+1}$ is the instantaneous photosynthetic rate of the next measurement point $t_i$ is the time recorded at the initial measurement point (h) $t_{i+1}$ is the time recorded at the next measurement point (h)
2	$W_{\text{CO}_2} = p \times 44/1,000$	$W_{\text{CO}_2}$ is the mass of $\text{CO}_2$ stored per unit leaf area ( $\text{g}\cdot\text{m}^{-2}\cdot\text{d}^{-1}$ ) 44 is the molar mass of $\text{CO}_2$
3	$W = W_{\text{CO}_2} \times L \times \text{Ca}$	$W$ is the daily carbon sequestration per plant ( $\text{g}\cdot\text{d}^{-1}$ ) $L$ is the leaf area index of the tree $\text{Ca}$ is the canopy area
4	$\text{Ca} = (\pi \times C_1 \times C_2)/4$	$\text{Ca}$ is the canopy area $C_1$ is the east–west width of the canopy $C_2$ is the south–north width of the canopy

approximately 20 s to allow them to match the evolving surroundings.

To make it shine straight on the leaves, the leaf chamber was lined up with the sunshine. Then, the value of the photosynthetic rate was monitored. The handle measurement button was pressed to record the data when the number stabilized. Every hour, for 1 hour, we recorded the photosynthetic rate values of 10–20 instantaneous leaves of the tree species, repeated it thrice, and computed the average value. The measurement period was from 9:00 a.m. until 4:00 p.m.

### 2.3.4.2 Calculation of carbon storage in plant communities

Drawing on past studies, methods such as photosynthetic stoichiometry and biomass analysis were used to estimate plant community carbon storage (Dong, 2013; Zhang, 2019; Yang et al., 2024). The specific methods are shown in Table 3. In this study, leaf carbon storage was calculated using the photosynthetic rate method; subsequently, the root, stem, and branch carbon storage were estimated using the biomass methodology.

TABLE 4 Biomass models of various tree species.

Species	Biomass models		Notes
<i>Ligustrum lucidum</i>	WA = 0.47118 × D <sup>1.64813</sup>	WB = 0.13282 × D <sup>1.47593</sup>	Zhang et al. (2018)
<i>Koelreuteria bipinnata</i>	WA = 0.12238 × D <sup>2.13793</sup>	WB = 0.00111 × D <sup>3.20022</sup>	Zhang et al. (2018)
	WT = 0.11478 × D <sup>2.06573</sup>	WL = 0.02068 × D <sup>1.68502</sup>	
<i>Populus</i>	WA = 0.019011 × D <sup>2.1051</sup>	WB = 0.001885 × D <sup>3.0213</sup>	Xue et al. (2014)
	WT = 0.013449 × D <sup>2.4535</sup>	WL = 0.003399 × D <sup>2.6815</sup>	
Other species	WT = 0.05549 × D <sup>2.87776</sup>	WB = 0.01124 × D <sup>3.16237</sup>	Wen (1997)
D ≤ 5 cm	WT = 0.11701 × D <sup>2.36933</sup>	WB = 0.01621 × D <sup>2.93859</sup>	
5 < D ≤ 10 cm	WT = 0.10769 × D <sup>2.34891</sup>	WB = 0.00385 × D <sup>3.15093</sup>	
10 ≤ D ≤ 20 cm	WT = 0.03541 × D <sup>2.65146</sup>	WB = 0.00583 × D <sup>2.94383</sup>	
D > 20 cm	WL = 0.07709 × D <sup>1.55399</sup>	WR = 0.01128 × D <sup>2.67850</sup>	

WA is the aboveground biomass model; WT is the stem biomass model; WB is the branch biomass model; WL is the leaf biomass model; WR is the root biomass model. In this study, only the biomass models of stem, branch, and root are included, whereas the leaf biomass is quantified using the photosynthetic rate method.

WT is a tree trunk biomass model; WB is a tree branch biomass model; WL is a leaf biomass model; WR is a tree root biomass model. Only the biomass models of tree trunk, branch, and root are addressed in this paper; the leaf component is evaluated using the photosynthetic rate method.

### 1. Optical contract quantification method

A photosynthesis meter measuring the instantaneous photosynthetic rate per unit leaf area of plant leaves was utilized to determine the overall change over a particular time. The technique (Dong, 2013), depending on the leaf area index of a single plant, is then used to determine the daily CS (DCS) of the particular plant.

DCS of several plants is shown in Table 3.

For estimating the DCS of plant groups utilizing the Rezwana (Sultana et al., 2021) technique for calculating carbon storage in urban GS plant communities, we utilized the DCS of plants. The Equation 2 is as follows:

$$C_{Sij} = C_{Aij} \times N_{Sij}. \quad (2)$$

In the equation,  $i$  is the specification,  $j$  is the tree species,  $C_{Sij}$  is the total DCS of the plant community,  $C_{Aij}$  is the DCS of trees or shrubs of this kind, and  $N_{Sij}$  is the number of trees or shrubs of this kind.

The DCS per unit area of a plant community is the ratio of the community's DCS to the plot area  $C_{ua} = C_{Sij}/S$ . Here,  $C_{ua}$  is the DCS per unit area of the green plant community and  $S$  is the area of the green plant community.

### 2. Biomass method

The biomass model of tree species with comparable climatic circumstances was used (Wen, 1997) as this study stresses the shrub and tree community (Table 4). Using basic plant knowledge—that is, the DBH value of particular tree species—the relevant biomass model may compute the biomass of the plant community. The formula is given in Equation 3:

$$B = 0.8 \times \frac{\sum B_i}{S}. \quad (3)$$

In the equation,  $B$  is the tree community's biomass, measured in kg/hm<sup>2</sup>;  $S$  is the sample plot's size, measured in hectares;  $B_i$  is the biomass; and 0.8 is the correction factor. Made up not only of a great

amount of organic material but also of water and a few minerals, the plant body is produced from the dry weight of plant organisms. Its fundamental composition largely consists of carbon, hydrogen, and oxygen; scholars at home and abroad often use an average carbon content of 0.5. The total biomass of plant communities provides the basis for the carbon storage computation as illustrated in Equation 4:

$$CS = B \times \alpha. \quad (4)$$

In the formula, CS represents the carbon storage, measured in kg C/hm<sup>2</sup>;  $B$  is the total biomass of the community, measured in kg C/hm<sup>2</sup>; and the value of  $\alpha$  is 0.5 (Fang et al., 2001).

### 2.3.5 Data analysis

Using SPSS software, a correlation study between several kinds of GS landscape pattern indices and carbon storage was conducted; urban GS carbon storage and community structure attribute factors' correlation and characteristic significance were then investigated using a combination of correlation and regression techniques.

### 2.3.6 Integration and complementary roles of remote sensing and field-based methods

Remote sensing and field methods are integrated in this study to allow multi-scaling in carbon storage assessment in urban green spaces, with the two methods assuming distinct but complementary roles.

The NDVI-derived model provides a macro-scale spatial overview of the AGC distribution, which is also available across the entire metropolitan area of Xi'an and captures broad patterns relating to GS coverage and landscape composition.

However, empirical correlations characterize this method, Table 5 illustrates urban green space AGC and carbon density of different vegetation coverage types in Xi'an, which lacks very fine structural and species-specific variations in vegetation. However, as for an area covered with the NDVI-derived model, field survey data collected from 40 representative plant communities in the Xi'an World Expo Park provide high-resolution views for biophysical

TABLE 5 Urban green space AGC and carbon density of different vegetation coverage types in Xi'an.

Type of coverage	Area (hm <sup>2</sup> )	Area percentage	AGC (×10 <sup>3</sup> )t	AGC percentage	Carbon density (kg/m <sup>2</sup> )
No coverage	16,169.88	19.38	—	—	—
Low coverage	22,044.79	26.42	46.29	7.33	0.21
Low-to-medium coverage	15,630.75	18.73	74.95	11.86	0.48
Medium coverage	11,240.40	13.47	109.94	17.40	0.98
Medium-to-high coverage	9,770.90	11.71	165.71	26.23	1.70
High coverage	8,591.29	10.30	234.87	37.18	2.73

drivers of CS DBH, planting density, and photosynthetic activity, for mechanistic understanding at the community level.

The field data are not directly used for calibrating the NDVI model due to spatial and temporal mismatch in the resolution of data, but they serve to validate and interpret the underlying ecological processes reflected in remotely sensed patterns. For instance, the demonstrated positive correlation between DBH and carbon storage helps explain why areas with mature tree cover have higher NDVI-based AGC values.

Hence, remote sensing is more suited for monitoring and planning of cities as a whole, whereas field-based assessments deal with finer scales of understanding micro-scale carbon dynamics, which can facilitate targeted management strategies.

Together, the two techniques form a synergistic framework: remote sensing identifies where carbon is stored and at what scale, whereas field surveys explain why and how it is stored, thereby enabling informed and multilevel urban GS planning for CS.

## 3 Results

### 3.1 Urban GS carbon storage space pattern

#### 3.1.1 Carbon storage in urban GSs

The metropolitan area of Xi'an in 2020 had 21,342.1 ha of GS, which was 35.57% of the total land. With an average density of 1.77 kg/m<sup>2</sup>, Figure 3 displays a total AGC of 376.97 tons. From the city core to the outskirts, the general carbon storage and carbon density exhibit a rising tendency. Urban parks, Chanba ecological wetlands, and Weihe ecological corridors mostly contribute to the high AGC and carbon density values in the study region; AGC is greater in the eastern half of the city than in the western section.

#### 3.1.2 Urban vegetation coverage

Among the low-coverage urban GSs in Xi'an city in the research region (Figure 4), 2020 had the highest at 26.42%, followed by no coverage, low-to-medium coverage, medium coverage, and medium-to-high coverage. Of the low-coverage urban GSs in Xi'an city across the study area (Figure 4), 2020 had the highest at 26.42%, followed by no coverage, low-to-medium coverage, medium coverage, and medium-to-high coverage. The least area had high coverage at 10.3%. The AGC distribution is most evident with 37.18% for high coverage and 26.23% for medium-high coverage; other kinds dip below 20%. High-coverage regions have

much greater carbon density than other categories, and because of their 10.3% area share, the aboveground carbon storage is the most significant component of the overall AGC.

#### 3.1.3 Layout of carbon storage spaces for multiple kinds of GSs

Different kinds of GSs have the following AGC performance: regional GS > affiliated GS > protective GS > park GS > square GS (see Table 6). Of the various kinds of GSs, regional GSs (311.97 × 103 kg) and affiliated GSs (39.15 × 103 kg) have the greatest AGC, with 82.7% and 10.39% of the overall AGC of urban GSs, respectively. Whereas square GSs have the lowest AGC (0.11 × 103 kg, 0.03%), park GSs (10.09 × 103 kg, 2.68%) and protected GSs (15.64 × 103 kg, 4.15%) are the next highest.

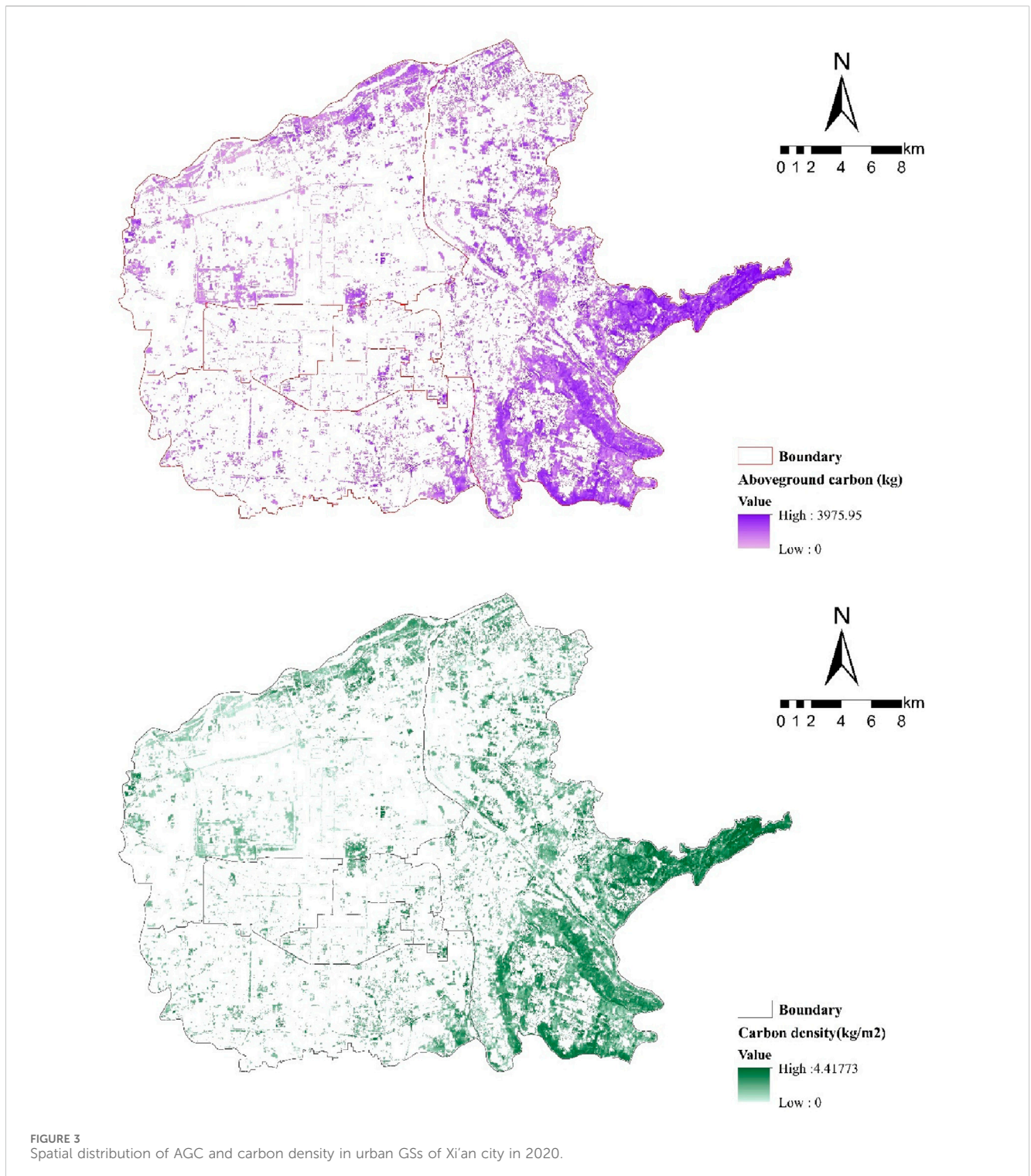
Among various kinds of GSs (Table 6), the carbon density varied greatly, especially between park GSs and protected GSs, square GSs ( $p < 0.05$ ), and protective GSs and square GSs ( $p < 0.05$ ). Regional GSs have the greatest carbon density at 1.99 kg/m<sup>2</sup>, park GSs come next at 1.22 kg/m<sup>2</sup>, and supplementary GSs were at 1.20 kg/m<sup>2</sup>. With carbon densities of 0.95 kg/m<sup>2</sup> and 0.77 kg/m<sup>2</sup>, respectively, protective GSs and square GSs had the least carbon density. The vast spread of regional GSs and park GSs mostly explains this.

Carbon density and carbon storage of several types of green ecosystems.

The findings of the analysis of variance ( $p < 0.01$ , Tables 2–3) revealed that regional GSs, which is much greater than other types of GSs, produced substantial variations in AGC across many forms of GSs. Although square GSs were much smaller than other kinds of GSs, carbon storage across protective GSs, supplementary GSs, and park GSs showed no notable difference.

### 3.2 Analysis of factors influencing carbon storage space in urban GSs

Research connected the AGC expected outcomes and landscape pattern indicators of many kinds of GSs. The findings of the study revealed a very notable positive link between urban GS AGC and CA, PLAND, as shown in Table 7. The more complicated the patches around the border, the more noticeable the "edge effect"; the bigger the AGC, the more efficient the CS. Looking at the landscape pattern index reveals that the regional GS with the most PLAND, with many huge patches and complicated borders, is the primary source of the amount of carbon storage in the spatial



pattern of the five types of GSs. Core patches have the lowest PD and landscape segmentation index; unit patches have the greatest LSI and LPI. Park GSs have an LPI that is second only to that of regional GSs; hence, the AGC of regional GS is the greatest. Although this sample is from a large metropolitan area with less GS and PLAND and less NP, hence lowering the AGC, the LPI of park GSs is second only to regional GSs. Although the PD and DIVISION of the protected GS are the highest, the AGC is somewhat low (Table 8).

### 3.3 The impact of plant community structure on sample carbon storage

In order to compare the carbon sequestration effects of different community types, based on the actual plant communities in the study area, 40 typical plant communities were divided into three types, namely, low-density, medium-density, and high-density, according to their planting density (Table 3) according to their planting density (Table 9).

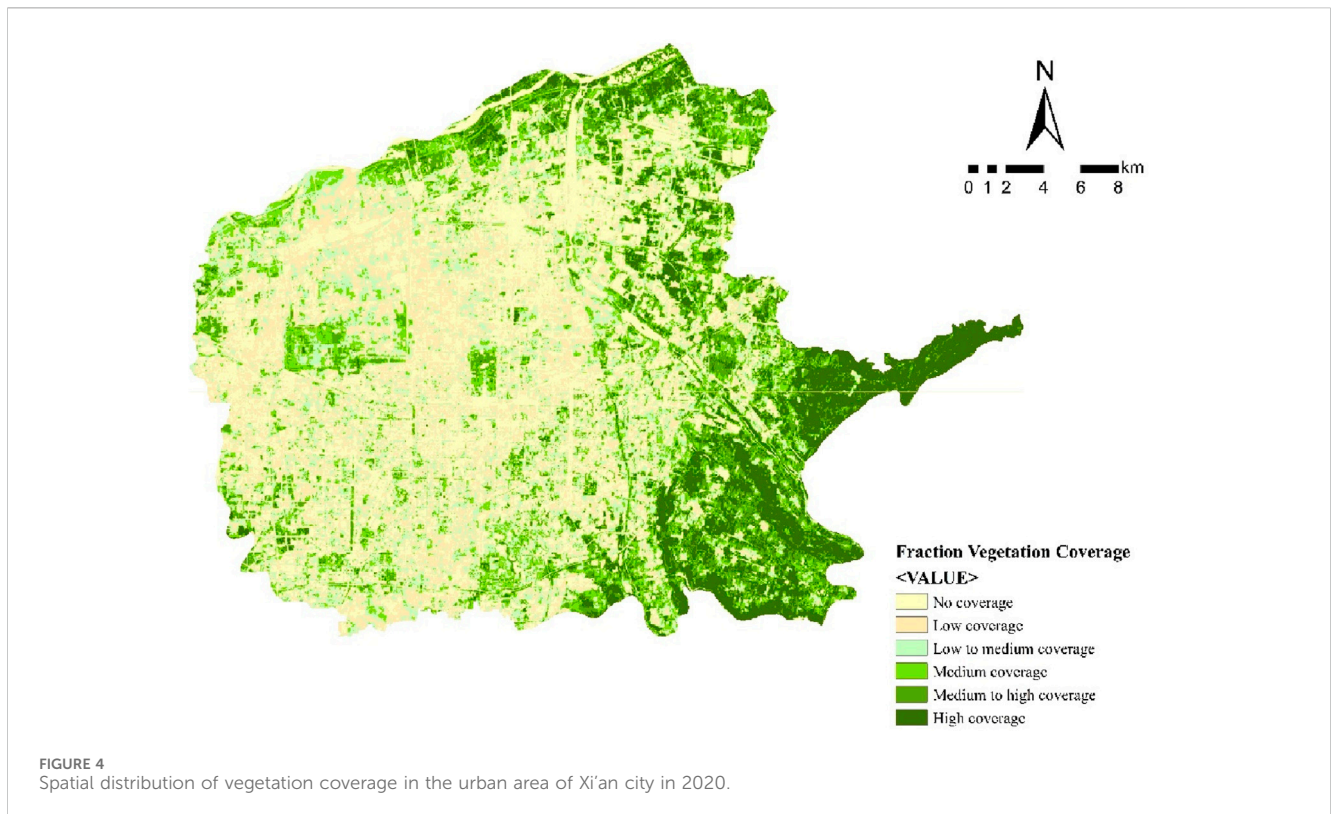


**TABLE 6** Statistical analysis of carbon storage and carbon density across different types of urban green spaces.

Category	Maximum		Minimum		Mean		Std. deviation	
	AGC (kg)	Carbon density (kg/m <sup>2</sup> )	AGC (kg)	Carbon density (kg/m <sup>2</sup> )	AGC (kg)	Carbon density (kg/m <sup>2</sup> )	AGC (kg)	Carbon density (kg/m <sup>2</sup> )
PS	2,858.7	3.14	0.03	0.01	846.31	0.95	539.93	1.43
AS	3,337.7	3.71	2.86	0.01	1,070.83	1.20	463.69	0.98
GS	2,970.3	3.30	1.568	0.01	1,115.38	1.22	515.47	1.25
SS	1,285.1	1.43	33.345	0.04	686.17	0.77	323.81	0.78
RS	3,975.9	4.42	0.065	0.01	1799.41	1.99	715.36	1.76

### 3.3.1 Carbon storage in plant communities of different density levels

Calculations revealed the DCS and carbon sequestration per unit area of plant communities as follows (Figure 5): high density > medium density > low density. High-density plant communities are characterized by a DCS of 186.72 g/m<sup>2</sup> and carbon sequestration per unit area of 25.7 kg/m<sup>2</sup>. Although medium and high densities reveal no visual difference, the analysis of variance revealed a significant difference ( $p < 0.05$ ) in the DCS per unit area of plant communities across low, medium, and high densities under different planting densities. Although medium and high densities show no noticeable difference, the difference in the carbon storage per unit area of plant communities under various planting densities is substantial ( $p < 0.05$ ) between low and high densities.

### 3.3.2 Analysis of carbon storage in plant communities of different density grades

Depending on various properties of varying density levels and DCS and storage, 40 plant communities were investigated (Table 10). From the viewpoint of various planting densities, in low-density plant communities, other variables are not linked with CS in the plant community, except for the crown width area and average DBH, which are strongly positively related to DCS and carbon storage in the plant community.

The DCS and carbon storage of the plant community in medium-density plant communities are considerably positively connected with the average plant height and average DBH. The DCS and carbon storage of the plant community in high-density plant communities show a notable positive correlation with the average DBH; the average plant height shows a notable positive correlation with the carbon storage per unit area.

TABLE 7 Correlation analysis of landscape pattern metrics and carbon storage for different green space types.

Landscape pattern index	AGC		Carbon density	Significance (P-value)
	Pearson correlation coefficient	Significance (P-value)	Pearson correlation coefficient	
CA	0.99**	0	0.946*	0.015
NP	0.58	0.304	0.595	0.29
PD	-0.65	0.23	-0.813	0.094
LPI	0.56	0.323	0.531	0.357
PLAND	0.99**	0	0.946*	0.015
FRAC	-0.258	0.676	-0.136	0.828
DIVISION	-0.556	0.331	-0.468	0.426
LSI	0.236	0.702	0.047	0.936

TABLE 8 Results of landscape pattern metrics calculation for various green space types.

	CA	NP	PD	LPI	PLAND	FRAC	SHAPE	DIVISION	LSI
GS	8.244	431	52.275	23.273	3.822	1.399	5.265	0.920	744.720
RS	157.807	5,147	32.616	30.924	73.157	1.396	4.905	0.873	72.207
SS	0.140	26	185.185	21.795	0.065	1.395	4.897	0.899	6.045
AS	32.761	5,387	164.434	2.437	15.187	1.395	4.735	0.997	80.976
PS	16.757	3,446	205.644	1.386	7.768	1.399	4.729	1.000	65.991

Area unit is km<sup>2</sup>.

TABLE 9 Division of planting density levels for plant communities.

Planting density levels	Density range (plants/m <sup>2</sup> )	Number of sample plots
Low planting density	0.025–0.065	12
Medium planting density	0.07–0.128	23
High planting density	0.13–0.235	5

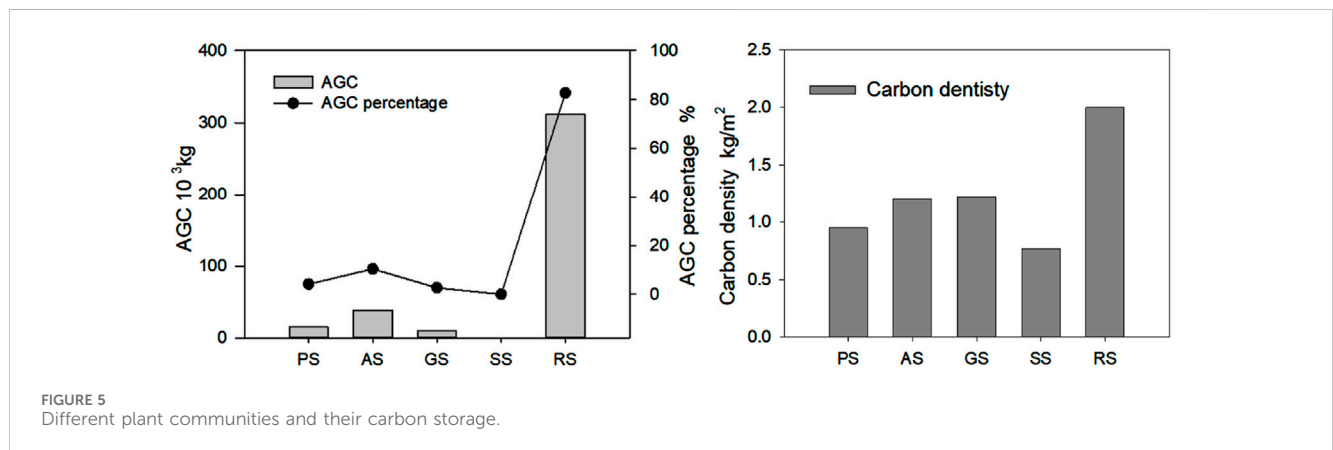


TABLE 10 Correlation of plant community characteristic factors and carbon storage.

Density type		Average height	Average DBH	Average crown width	Canopy closure	Proportion of evergreen and deciduous	Tree density	Plant community density
Low density	DC	0.33	0.143	0.648*	0.178	0.216	-0.488	-0.286
	CC	0.551	0.826**	0.177	-0.479	0.312	0.283	0.019
Medium density	DC	0.458*	0.582**	0.022	0.322	0.063	-0.162	0.106
	CC	0.652**	0.782**	0.007	0.265	-0.426*	0.363*	0.320
High density	DC	0.138	0.282**	0.566	0.181	0.389	0.278	0.674
	CC	0.894*	0.962**	-0.325	0.843	-0.103	0.787	0.684
All types	DC	0.413**	0.38*	0.026	0.31*	0.111	0.073	0.328*
	CC	0.458**	0.526**	-0.069	0.179	-0.013	0.473**	0.565**

DC is the daily carbon sequestration per unit area ( $\text{g CO}_2/\text{m}^2$ ) and CC is the carbon storage per unit area ( $\text{kg C}/\text{m}^2$ ).  
Outside 3–4 correlation of plant community characteristic factors and carbon storage.

The crown width area is strongly positively related to the DCS per unit area of low-density plant communities; it is not so for other kinds of plant communities. The DCS per unit area is strongly positively correlated with the average DBH; in most cases, the average plant height is also strongly positively correlated with the average DBH; tree density is strongly positively correlated with the carbon storage per unit area of medium-density plant communities; the proportion of deciduous trees is strongly negatively correlated with carbon storage in medium-density plant communities but not with other community types.

The average plant height, average DBH, and community planting density across all plant community types show significant positive correlation with DCS and carbon storage in the community; the crown area and the ratio of evergreen to deciduous trees show no correlation with DCS and carbon storage in the community.

### 3.3.3 Regression analysis of carbon storage in plant communities

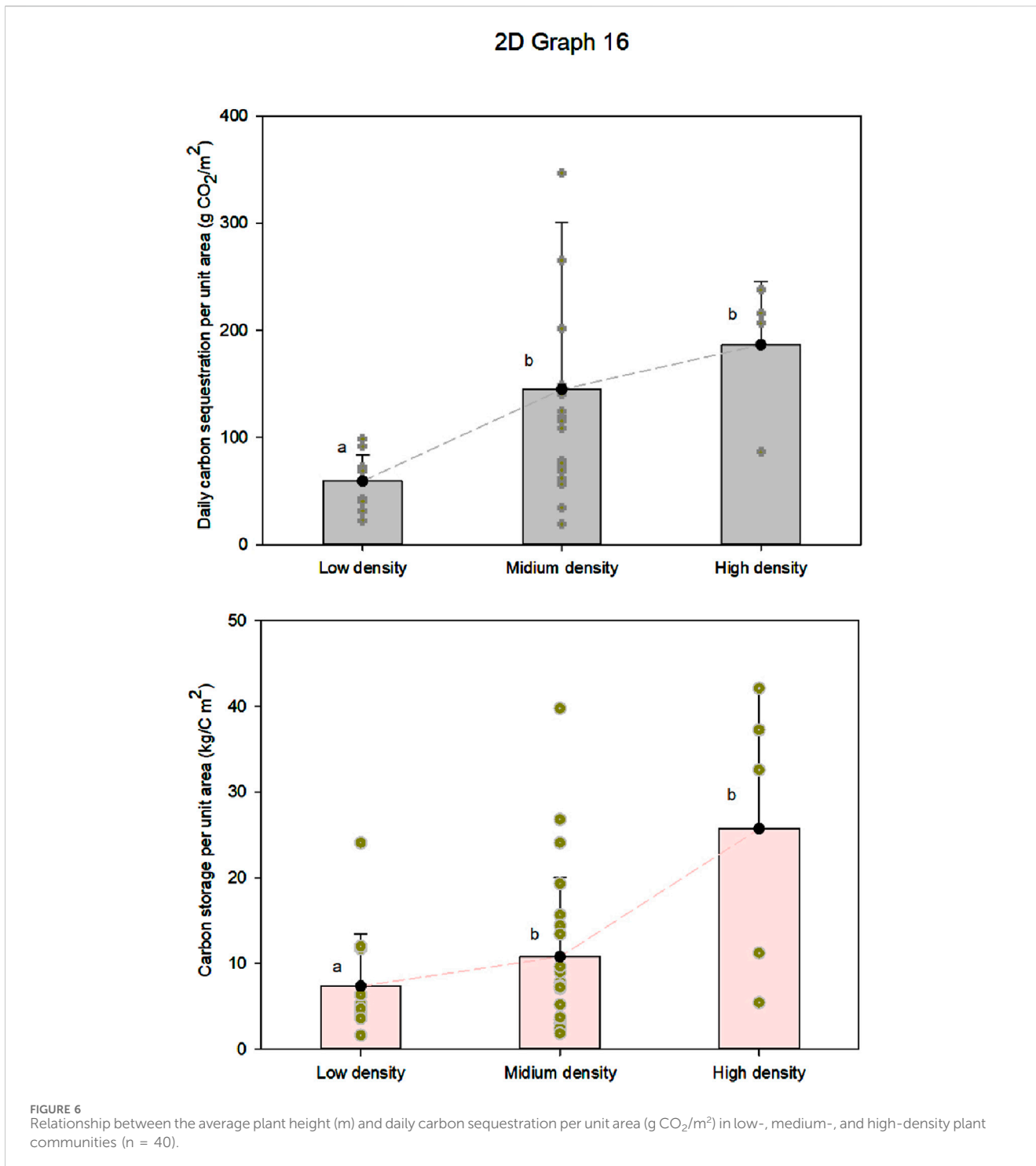
Using the diameter structure and planting density as independent variables from the above-described correlation study, nonlinear formula fitting regression on CS in several plant communities was conducted. The power equation was found to be the model for the average plant height, daily carbon sequestration, and carbon storage based on the regression results of the diameter structure and CS after assessing significance and  $R^2$ ; the power equation as the average DBH and daily carbon sequestration; and the logarithmic equation as the model for unit area carbon storage. The power equation, derived from the regression findings of community density and carbon sequestration, was used to simulate community density and daily carbon sequestration. Community density and carbon storage were modeled using cubic regression (Figures 10, 11).

Results in Figure 6 reveal that for daily carbon sequestration, the fitting effect between the average plant height and DCS in the three kinds of plant communities is quite low, with  $R^2$  below 0.3, suggesting a poor fitting effect for high-density plants. Increasing the average plant height also increases the DCS per unit area of plant communities. Among the three categories of plant communities in terms of carbon storage, high-density simple linear fitting beats with

an  $R^2$  of 0.79; low-density fitting falls short with an  $R^2$  of 0.4. Increasing the average plant height increases the carbon storage per unit area of plant communities. Previous studies indicate that a higher plant height will help to increase the DCS and unit area carbon storage, hence enhancing the CS of plant communities.

DCS and the average breast height diameter regression analysis (Figure 7) show that medium-density simple linear fitting among the three plant community types performs the best, with an  $R^2$  of 0.34. The DCS increase per unit area of plant communities coincides with the average DBH growth. The three kinds of plant communities' simple linear fitting impact on carbon storage (Figure 8) is considerable, with  $R^2$  more than 0.5; high-density fitting has the biggest influence, with  $R^2 = 0.93$ . Generally speaking, the carbon storage per unit area of plant communities increases with the increasing average DBH, and the growth trend exhibits a progressively slowing pattern. Studies have shown that although the development slows down between 30 and 40 cm, the carbon storage per unit area of plant communities increases quickly when the average DBH grows between 10 and 30 cm. Our findings indicate that increasing the average height of plants does not increase the DCS of plant communities.

Among the three plant community types in the regression analysis of plant community density and unit area carbon storage (Figure 9), the open type, with an  $R^2$  of 0.4, exhibited the most significant simple linear fitting effect. From an overall perspective (Figure 9), the study found an S-curve change in the DCS of plant communities as the plant community density increased. When the community density was between 0.02 and 0.13  $\text{no}/\text{m}^2$ , the daily carbon sink per unit area of plant communities increased rapidly with increasing community density. When the tree density dropped between 0.13 and 0.23  $\text{no}/\text{m}^2$ , the daily carbon sink per unit area of plant communities increased slowly with the increase in tree density. Among the three plant community types, the regression analysis of plant community density and unit area carbon storage (Figure 10) reveals that the medium-density community's simple linear fitting effect is the best. Research has shown that when the plant community density increases, the carbon storage per unit area of plant communities shifts along a curve. When tree density is between 0.02 and 0.05  $\text{plants}/\text{m}^2$ , the



carbon storage per unit area of plant communities diminishes with increasing plant community density; it remains in the range of 7 g/m<sup>2</sup>–10 g/m<sup>2</sup>. When the plant community density is 0.05 plants/m<sup>2</sup>–0.22 plants/m<sup>2</sup>, the carbon storage per unit area increases from 10 g/m<sup>2</sup> to approximately 30 g/m<sup>2</sup> with the increase of plant community density. When the tree density of the plant community exceeds 0.22 plants/m<sup>2</sup>, the increase in plant community density causes the development of the carbon storage per unit area to stall.

## 4 Discussion

### 4.1 Carbon storage capacity of GSs in Xi'an city

A significant component of urban carbon sinks, urban GSs, exhibit remarkable spatial variation in carbon storage and density all around (Nowak et al., 2013; Strohbach et al., 2012). The factors include climatic conditions, urbanization development, kinds of

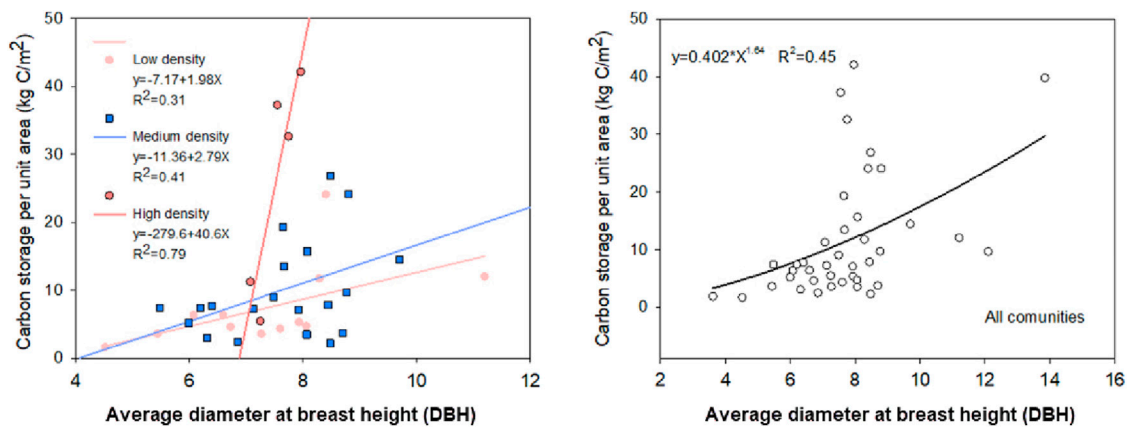


FIGURE 7 Relationship between the average plant height (m) and carbon storage per unit area (kg C/m<sup>2</sup>) in plant communities of varying density levels.

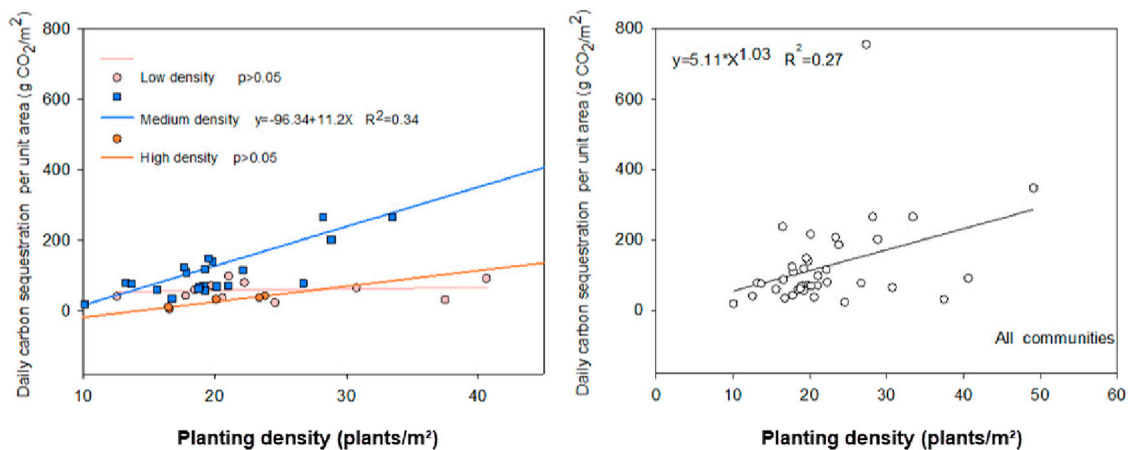


FIGURE 8 Regression analysis of the average diameter at breast height (DBH) (cm) and daily carbon sequestration per unit area (g CO<sub>2</sub>/m<sup>2</sup>).

GSs, and urban management practices that lead cities to differ substantially in the ratio of GSs carbon storage to total carbon storage (Zhao et al., 2023; Fan et al., 2022; Wang et al., 2021). Earlier studies (Strohbach et al., 2012; Liu and Li, 2012; Wang et al., 2021) indicate that cities with higher carbon density are Sydney (1.74 kg C/m<sup>2</sup>), New York (1.68 kg C/m<sup>2</sup>), and Beijing (1.52 kg C/m<sup>2</sup>), largely as a result of increased green cover and a large number of urban parks. Averaging 1.77 kg/m<sup>2</sup>, Xi'an's urban GS system in 2020 sequestered 376.97 tons of carbon, which is much less than that of other cities. The Xi'an urban GS's relatively low overall coverage, which is influenced by climatic factors such as precipitation and urbanization development, is the main reason.

According to the present study, both arbitrarily constituted green spaces (AGS) and protective green spaces (PGS) have low carbon densities compared to most other types of carbon storage areas.

The only drawback with this research is that the argument that landscape connectivity might improve their carbon sequestration potential is based primarily on indirect landscape pattern metrics such as DIVISION and PD, which indicate high fragmentation and isolation in these GS types. Because of the limitations in high-resolution movement or ecological flow data for urban vegetation, the current analysis did not include direct quantitative evidence linking connectivity to carbon density; for example, functional connectivity models or spatial autocorrelation analyses. Figure 11 illustrates the relationship between the average plant height (m) and carbon storage per unit area (kg C/m<sup>2</sup>) in plant communities of varying density levels.

However, the negative correlation between DIVISION and carbon density across GS types (Table 7) was not statistically significant when viewed for AGS and PGS alone due to sample constraints, yet it conforms to established ecological principles; fragmented patches usually experience edge effects,

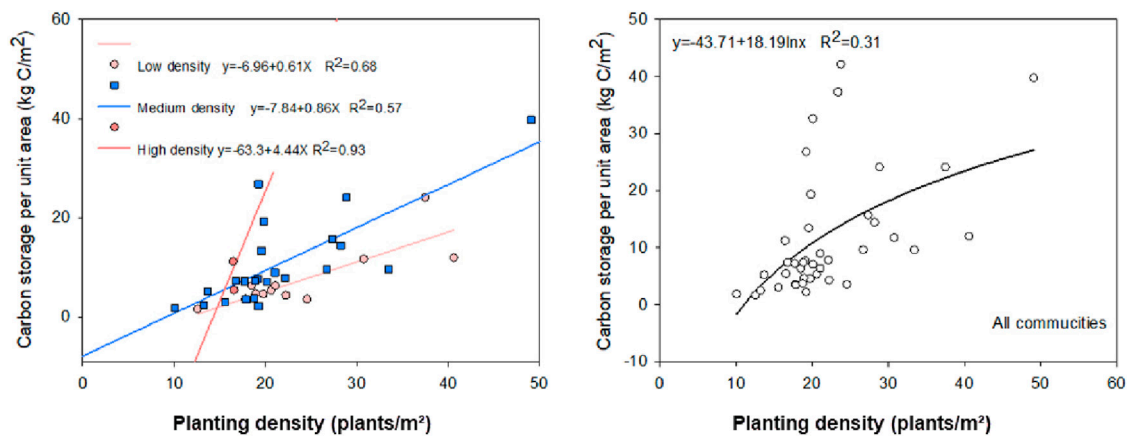


FIGURE 9 Relationship between the average DBH (cm) and carbon storage per unit area ( $\text{kg C/m}^2$ ), showing the power-law trend with  $R^2$  values for each density group.

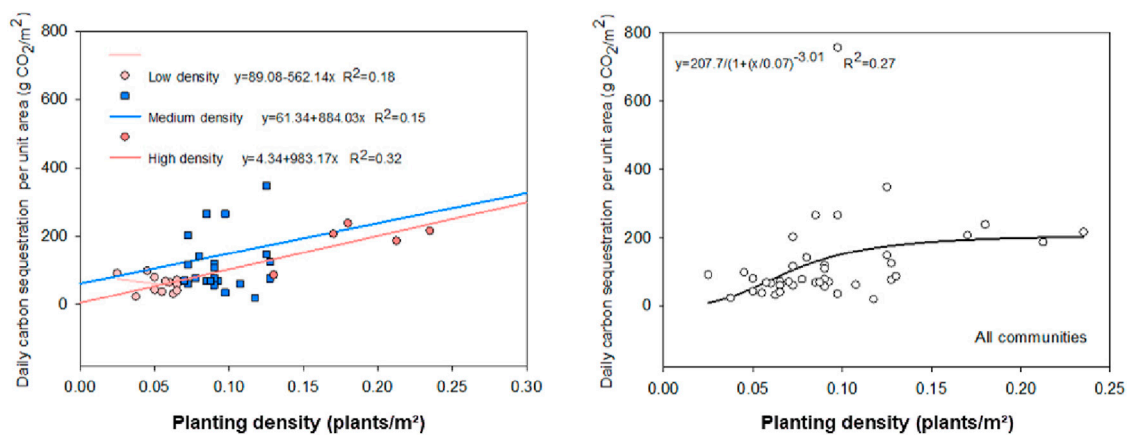


FIGURE 10 Effect of the planting density ( $\text{plants/m}^2$ ) on daily carbon sequestration per unit area ( $\text{g CO}_2/\text{m}^2$ ), illustrating an S-shaped curve trend.

microclimatic stress, and low ecological resilience, which restrain biomass accumulation, thus decreasing the carbon storage potential. In support of this, previous research showed evidence for connected GSs facilitating good tree growth, diversity, and long-term stability of vegetation, which, taken together, result in increased carbon sequestration (Nowak et al., 2013; Chen et al., 2024).

For example, Chen et al. (2024) showed that GSs of contemporary values in cities store carbon more efficiently than constructed small patches of comparable size, with efficiencies reaching 18%.

Although these authors were not able to carry out direct modeling of connectivity impacts, somewhat integrated landscape pattern analysis and findings from the existing literature represent the best reasonable ground for recommending the enhancement of spatial connectivity between small-scale GSs to enhance their CS efficiency.

The examined area reveals an uneven distribution of GS AGC in Xi'an city. Most of the medium, medium-high, and high coverage areas are in the Chanba region or park GSs, which creates a spatial distribution of high carbon storage around the periphery and low in the core of Xi'an city. Conversely, urbanization has led to consistent construction and hard surface cover on the ground in the city center, hence lowering plant cover. Only in areas with significant plant density, including parks and GSs, can high carbon storage sites be discovered. On the outskirts of the city, where the plant cover is considerable, low development intensity has resulted in a vast number of new parks and regional GSs being constructed. Its significant carbon storage increases the AGC on the outskirts of the city as well. Thus, the more the plant cover, the higher the aboveground carbon storage and carbon density. A good approach is thought to be increasing the carbon storage capacity of urban plants using increased urban GS coverage.

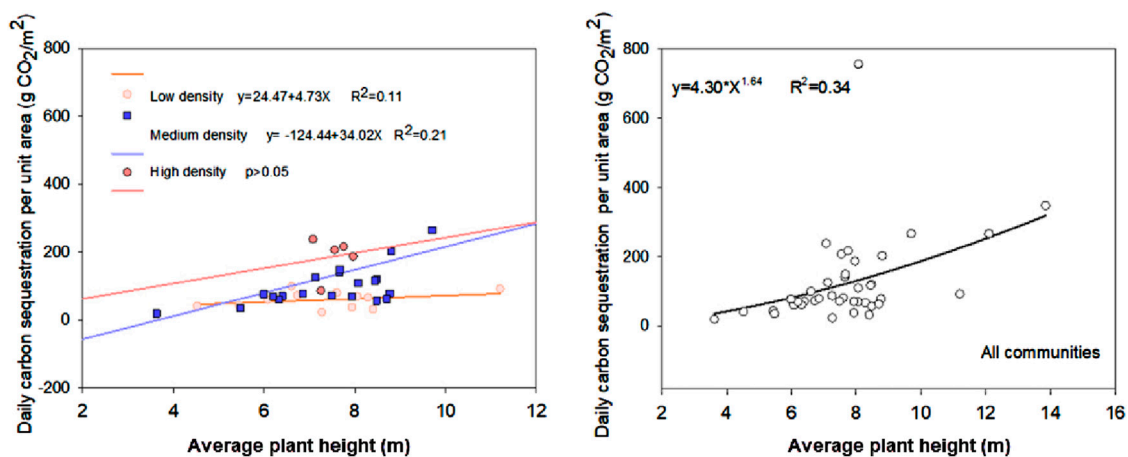


FIGURE 11 Relationship between the planting density (plants/m<sup>2</sup>) and carbon storage per unit area (kg C/m<sup>2</sup>), showing cubic regression fitting by density class.

## 4.2 The impact of different types of GSs on the AGC distribution of urban GSs in Xi'an

Urban GS carbon storage is highly influenced by many distinct types of GS carbon storage. The main carbon sink for urban GSs is the carbon storage of urban forests. More than 80% of the carbon storage in urban GSs is provided by North American urban forests (Nowak et al., 2013). Park GSs in Sheffield, United Kingdom, make up 40% of the carbon storage of urban GSs (Davies et al., 2011). On the other hand, studies have shown that recommending GS design optimization strategies for different kinds of GSs might boost the CS capability of other GSs. Although their carbon density is lower than that of other types of GSs, Chen et al.'s 2024 study showed that connected GSs make up 56% of carbon storage to 65% of the GS area. Examining the plant structure and the traits of many AGS kinds in conjunction with the recommendation of several optimization design options for different GS types might help to maximize the potential of AGS. The results show that although regional GSs and associated GSs have more overall AGC for Xi'an city than park GSs and regional GSs, the latter have more carbon density. The spatial distribution of carbon storage in urban GSs is influenced by the city size, GS coverage, and management practices (Nowak et al., 2013; Zhao et al., 2023; Liu and Li, 2012). Different types of GSs should be studied without delay, along with optimization strategies to boost the AGS carbon storage.

Although the current study identifies that AGS and PGS exhibit relatively low carbon density despite contributing significantly to total carbon storage, the suggestion that enhancing landscape connectivity could improve their carbon sequestration potential is primarily based on indirect landscape pattern metrics such as DIVISION and PD, which indicate high fragmentation and isolation in these GS types. Direct quantitative evidence linking connectivity to carbon density—such as functional connectivity models or spatial autocorrelation analyses—was not included in this study due to limitations in high-resolution movement or ecological flow data for urban vegetation. However, the observed negative correlation between DIVISION and carbon density across GS types (Table 7), although not statistically significant for AGS and PGS alone due to sample constraints, aligns

with established ecological principles; fragmented patches often experience edge effects, microclimatic stress, and reduced ecological resilience, all of which can limit biomass accumulation and carbon storage capacity. This interpretation is supported by prior research showing that connected GSs facilitate improved tree growth conditions, species diversity, and long-term vegetation stability, thereby enhancing CS (Nowak et al., 2013; Chen et al., 2024). For instance, Chen et al. (2024) demonstrated that structurally connected GSs in urban settings increased carbon storage efficiency by up to 18% compared to isolated patches of similar size. Therefore, while direct modeling of connectivity effects is beyond the current scope, the integration of landscape pattern analysis with findings from existing literature provides a reasonable basis for recommending improved spatial linkage among small-scale GSs as a strategy to enhance their CS performance.

Multiple kinds of the GS landscape design affect urban GS carbon storage. Generally, increasing the GS size will increase the CS capacity of GSs (Wang and Shi, 2015). The CS was also much higher than that in other GSs, as the regional GS and its share of the total GS in this study were far larger than that of other GSs. Their size closely relates to the higher carbon storage of protected GSs and other GSs. However, for areas with low GS percentages, it is advised that the GS size be increased. Given the geographical spread of the carbon storage in Xi'an urban GS in this study, it is recommended to stress the layout of larger park GSs in the core region. Low carbon density results from the uneven distribution of supplemental and protective GSs, as well as inadequate fragmentation of GSs. Considering the interaction between small and micro GSs as additional GSs is also rather important when designing a compact, spatially organized GS as a whole.

## 4.3 The influence of plant community structure properties on CS indicators

Park GSs are significant carbon sinks in the majority of cities, typically accounting for 20%–35% of urban GS carbon storage (Davies et al., 2011; Zhao et al., 2023; Wang et al., 2021). The composition of tree species, vegetation structure, and human

management methods are the primary factors contributing to the high carbon storage in park GSs. Consequently, it is imperative to assess them independently of the attributes and structure of the vegetation.

This study looked at the relationship between carbon storage in typical plant communities and other markers of associated vegetation structure and characteristics. The results revealed a notable link between carbon storage in typical plant communities and measures of vegetation structure and traits in the study area. The main factors of community carbon storage were the average plant height, average DBH, and community density, which correspond with other findings. Trees' capacity for CS is significantly influenced by their age and physiological state. Research has shown that young trees develop quickly and fix more carbon per unit time; nevertheless, their size is tiny, and their total carbon storage capacity is restricted. Conversely, elder trees may store more carbon because of their notable biomass even if their annual growth is declining (Stephenson et al., 2014; Nowak et al., 2013). There is a notable positive correlation between the mean DBH and carbon storage. Increasing tree biomass directly enhances the potential for carbon sequestration, hence increasing the carbon storage capacity as the DBH grows (Nowak et al., 2013). Nevertheless, the interaction between the two is not totally clear-cut. Stephenson et al. (2014) demonstrated that the marginal increase of carbon storage slows when the DBH reaches a certain threshold, hence generating a power function or logarithmic curve growth pattern. According to Gülçin and Cecil. (2021), trees in the 20 cm–40 cm diameter range, which make up 60% of the total, are largely responsible for the carbon storage of campus GSs. The rate of carbon storage accumulation decreases as the DBH surpasses 45 cm. The rate of biomass growth decreases and the carbon storage stabilizes when trees' DBH reaches a certain standard, hence clarifying this. The total CS of plant communities is substantially influenced by the density of the community plants (Zhang et al., 2024). Under the same circumstances, higher density will directly improve biomass and CS. Research has shown that when the density of plant communities increases, so does their CS rate; moreover, there is a very significant positive link between the carbon density of the community and the CS rate (Yang et al., 2024; Zhao et al., 2023; Liu and Li, 2012). Based on their research, Yi and Wang. (2019) discovered that the CS of sites with varying planting densities per unit area is not always preferable. Medium-density plots store more carbon than high-density and low-density plots. This work's daily CS and planting density revealed an S-shaped curve. Daily carbon sink per unit area of the plant community increased gradually with increasing tree density when the seeding density fell between 0.13 and 0.23 plants/m<sup>2</sup>. Increasing the plant density per unit area appeared to enhance the community's total carbon fixation capacity. On the other hand, high density might impede the development of plant communities by generating resource limitation and competition for light. Plants thrive in low-resource environments, including water, temperature, light, and space. Members of the plant community create mutual challenges and boundaries among themselves to get the most appropriate environmental resources for their growth. High planting density may squeeze the trees' growing area and increase mortality rates. Thus, the selection of an appropriate planting density for the community might increase the photosynthetic intensity in the plants, enhance the biomass of the flora, and eventually increase the carbon storage of the plant community.

#### 4.4 Urban GS design and regulation of the plant community structure to enhance carbon sequestration

To maximize the CS potential of GS systems, the GS design should take into account the whole quantitative relationship between spatial landscape patterns and carbon storage in different kinds of GSs. Among urban GSs, regional GSs, which have a high percentage of plant cover, good connectivity, and large GSs, provide the most carbon storage. The site exhibits degraded green space (GS) functions, relies on single-plant planting types, and suffers from poor connectivity among protective green spaces. The impermeable area is very large and the degree of fragmentation is notable even if the number of connected GSs is the highest. Among the park's most remarkable features are its vast GS, varied species, and high carbon-storage capacity per unit area. Usually made up of single-layer tree planting methods and a lot of hard surfaces, square green landscapes have little plant cover. There are no multilayered tree, shrub, and grass planting plans. Therefore, improving the connection of the whole landscape pattern from the viewpoint of the landscape pattern index study is very crucial if urban GSs are to have more CS capacity. Apart from raising the general carbon storage capacity of urban ecosystems, it might lower the patch separation index, reduce the problem of habitat fragmentation in cities, and increase the patch area.

RS: reduce the impact of the urbanization process and increase high-CS tree species. PS: increase the connectivity of GSs, avoid single-level planting, and ensure the health of trees.

AS: increase the proportion of high carbon-storage species and vertical greening in GSs, improve tree management and maintenance, and enhance CS capacity per unit area. GS: increase the GS of central urban parks or increase their vegetation coverage, add high-CS tree species, and reduce human interference.

SS: optimize the design of the multilayered community structure, increase the proportion of shrubs, and reduce the impermeable area.

The optimization of the DBH structure of trees in urban GSs is also advocated in this study to guarantee that the community structure is made up of tree species with different diameter classes, therefore raising the proportion of trees with a DBH in the 20 cm–40 cm range. The dual goals of species diversity and carbon storage can be attained in urban settings with limited GS resources by choosing suitable community planting densities, boosting the multilayered planting structure of trees and shrubs, and maximizing the CS capacity of plant communities.

The criticisms or the points highlighted as suggestions in the valuable feedback of the reviewers have indeed contributed significantly toward improving the methodological clarity and the scientific basis of the study.

In order to respond to those, the specific paragraphs on the integration and way each approach, that is, remote sensing and ground survey, complementing the others, have been revised to explicitly state that NDVI-based models offer a macroscopic spatial perspective of the AGC distribution across Xi'an, whereas field surveys provide microscopic mechanistic insights into plant community structure and CS processes.

Direct calibration of the NDVI model with field data was restricted by spatial and temporal differences. Field observations, however, interpret and validate the ecological patterns reflected in the remote-sensing results.

Moreover, in addition to strengthening the case regarding landscape connectivity and carbon storage in small-scale GSs (e.g., accessory and protective GS), we extended the discussion with indirect quantitative support, for example, a negative correlation trend between the DIVISION and carbon density, and added recent evidence showing increased carbon sequestration in connected GSs.

Finally, standardization of all cross-city carbon density values in a uniform unit of measurement ( $\text{kg C/m}^2$ ) has enabled valid comparisons to be made: Xi'an's average carbon density ( $1.77 \text{ kg/m}^2$ ) is now compared with that of Beijing ( $1.52 \text{ kg/m}^2$ ) and New York ( $1.68 \text{ kg/m}^2$ ), showing that Xi'an performs slightly better—all this while recognizing differences in GS typology and sources of data. In summary, these revisions together increase the methodological lucidity, analytical rigor, and general applicability of our findings for urban carbon management.

An important aspect of carbon dynamics in urban GS reviewed in this paper is carbon storage variation across different GS types and the impact of plant community structure on sequestration efficiency. In response to the reviewers' concerns, the manuscript has been improved in three important aspects to support the rationale with higher methodological rigor and greater scientific clarity.

First, by clearly specifying the complementary roles of both remote-sensing and field methodologies, we specify how the NDVI-derived models provide macro-level spatial assessments of the AGC distribution across the entire metropolitan area, whereas the field surveys in the Xi'an World Expo Park provide micro-mechanistic insight into how structural traits such as DBH or planting density impact carbon storage.

Although direct model calibration was limited by spatial mismatches, the field data serve to interpret and validate the ecological patterns observed in the remote-sensing results. Second, we have added indirect quantitative evidence—an observed negative trend between DIVISION and carbon density—to strengthen the argument linking landscape connectivity to CS in small-scale GSs (e.g., accessory and protective GS), along with recent literature showing that ecologically connected GSs enhance carbon storage.

Finally, we have standardized all intercity comparisons on one common unit ( $\text{kg C/m}^2$ )—Xi'an's average of  $1.77 \text{ kg/m}^2$  was thereafter compared with  $1.52 \text{ kg/m}^2$  for Beijing and  $1.68 \text{ kg/m}^2$  for New York, revealing that although Xi'an was slightly better off, the authors still insist on the fact that this is contextualized with differences in the definition of GS and, hence, the methodology. The revisions made in this manuscript aid in improving the transparency, comparability, and wider applicability of our findings for urban carbon-management strategies.

## 5 Conclusion

Rapidly urbanizing cities and limited urban land resources are demanding increasing requirements of urban GSs in urban ecosystems. In this study, we thoroughly investigated the CS capacity of GS systems in the Xi'an metropolitan area from the perspectives of urban landscape design and plant communities. Changes in urban GS functions and plant cover have a major impact on the AGC and carbon density of

many kinds of GSs. Urban land space is restricted; hence, sensible design strategies assist in optimizing the CS effect of urban GSs. Thus, we looked at the landscape patterns of various GSs and suggested several optimization design concepts to best use the AGS potential. Furthermore, aided by a comprehensive field survey, in this study, we assessed the link among carbon sequestration, plant community structure, and vegetation features. Several structural components intended to enhance the CS capacity of urban GSs and assist the sustainable development of the urban ecological system were also proposed.

## Data availability statement

The original contributions presented in the study are included in the article/Supplementary Material; further inquiries can be directed to the corresponding author.

## Author contributions

XW: Conceptualization, Formal analysis, Investigation, Methodology, Project administration, Resources, Writing – original draft, Writing – review and editing. WX: Investigation, Writing – original draft, Writing – review and editing. YR: Investigation, Writing – original draft, Writing – review and editing. MC: Investigation, Writing – original draft, Writing – review and editing. SM: Investigation, Writing – original draft, Writing – review and editing.

## Funding

The author(s) declare that financial support was received for the research and/or publication of this article. This study was supported by the Natural Science Basic Research Plan in Shaanxi Province of China (Program No. 2023-JC-YB-211), the Forestry Science and Technology Innovation Project of Shaanxi Province (Program No. SXLK2023-02-17), and the Institutional Funds of Yangling Vocational and Technology College (Program No. BG2021001).

## Conflict of interest

The authors declare that the research was conducted in the absence of any commercial or financial relationships that could be construed as a potential conflict of interest.

## Generative AI statement

The author(s) declare that no Generative AI was used in the creation of this manuscript.

Any alternative text (alt text) provided alongside figures in this article has been generated by Frontiers with the support of artificial intelligence and reasonable efforts have been made to ensure accuracy, including review by the authors wherever possible. If you identify any issues, please contact us.

## Publisher's note

All claims expressed in this article are solely those of the authors and do not necessarily represent those of their affiliated

organizations, or those of the publisher, the editors and the reviewers. Any product that may be evaluated in this article, or claim that may be made by its manufacturer, is not guaranteed or endorsed by the publisher.

## References

- Chen, L. S., Wang, Y., Zhu, E. Y., Wu, H. F., and Feng, D. L. (2024). Carbon storage estimation and strategy optimization under low carbon objectives for urban attached green spaces. *Sci. Total Environ.* 923, 171507. doi:10.1016/j.scitotenv.2024.171507
- Davies, Z. G., Edmondson, J. L., Heinemeyer, A., Jonathan, R., and Gaston, K. J. (2011). Mapping an urban ecosystem service: quantifying above-ground carbon storage at a city-wide scale. *J. Appl. Ecol.* 48 (5), 1125–1134. doi:10.1111/j.1365-2664.2011.02021.x
- Dong, Y. M. (2013). *Carbon sequestration benefit assessment and application research of 57 landscape tree species in huagangguanyu park*. Hangzhou: Zhejiang A&F University.
- Fan, L. Y. X., Wang, J. M., Han, D., Gao, J., and Yao, Y. Y. (2022). Research on promoting carbon sequestration of urban green space distribution characteristics and planting design models in Xi'an. *Res. Promot. Carbon Sequestration Urban Green Space Distribution Charact. Plant. Des. Models Xi'an. Sustain.* 15 (1), 572. doi:10.3390/su15010572
- Fang, J. Y., Pao, S. L., and Zhao, S. Q. (2001). The Carbon Sink: the role of the middle and high latitudes terrestrial ecosystems in the northern hemisphere. *Acta Phytoecol. Sinica* (05), 594–602.
- Gülçin, D., and Cecil, C. (2021). Assessment of above-ground carbon storage by urban trees using LiDAR data: the case of a university campus. *Forests*. 12 (1), 62. doi:10.3390/f12010062
- Hausfather, Z., Marvel, K., Schmidt, G. A., Nielsen-Gammon, J. W., and Zelinka, M. (2022). Climate simulations: recognize the 'hot model' problem. *Nature* 605, 26–29. doi:10.1038/d41586-022-01192-2
- Jiang, L. H. (2021). Global carbon cycle: from fundamental scientific problem to green responsibility. *Science* (1), 39–43.
- Liu, C. F., and Li, X. M. (2012). Carbon storage and sequestration by urban forests in Shenyang, China. *Urban For. & Urban Green.* 11 (2), 121–128. doi:10.1016/j.ufug.2011.03.002
- Nowak, D. J., and Crane, D. E. (2002). Carbon storage and sequestration by urban trees in the USA. *Environ. Pollut.* 116 (3), 381–389. doi:10.1016/s0269-7491(01)00214-7
- Nowak, D. J., Greenfield, E. J., Hoehn, R. E., and Lapoint, E. (2013). Carbon storage and sequestration by trees in urban and community areas of the United States. *Environ. Pollut.* 178, 229–236. doi:10.1016/j.envpol.2013.03.019
- Seto, K. C., Guneralp, B., and Hutyra, L. R. (2012). Global forecasts of urban expansion to 2030 and direct impacts on biodiversity and carbon pools. *PNAS* 109 (40), 16083–16088. doi:10.1073/pnas.1211658109
- Shi, T. M., Wang, D., Tang, Y., Li, P. Y., and Chu, Y. Q. (2023). Research progress on calculation method and impact factors of carbon sequestration capacity in urban ecosystems. *Chin. J. Appl. Ecol.* (02), 555–565.
- Stephenson, N. L., Das, A. J., Condit, R., Russo, S. E., Baker, P. J., Beckman, N. G., et al. (2014). Rate of tree carbon accumulation increases continuously with tree size. *Nature* 507, 90–93. doi:10.1038/nature12914
- Strohbach, M. W., Arnold, E., and Haase, D. (2012). The carbon footprint of urban green space—a life cycle approach. *Carbon Footpr. urban green space-A life cycle approach. Landsc. Urban Plan.* 104 (2), 220–229. doi:10.1016/j.landurbplan.2011.10.013
- Sultana, R., Ahmed, Z., Hossain, M. A., and Begum, B. A. (2021). Impact of green roof on human comfort level and carbon sequestration: a microclimatic and comparative assessment in Dhaka City, Bangladesh. *Urban Clim.* 38, 100878. doi:10.1016/j.uclim.2021.100878
- Velasco, E., Roth, M., Tan, S. H., Quak, M., and Norford, L. (2016). *The role of vegetation in the CO<sub>2</sub> Flux a Trop. urban park. Landsc. Urban Plan.* 148, 99–107. doi:10.1016/j.landurbplan.2015.12.003
- Wang, D. S. (2009). Research on the measurement of garden plant biomass in Beijing urban area. *For. Resour. Manag.* (04), 120–125.
- Wang, M., and Shi, Q. S. (2015). A study of influencing factors to urban green carbon sequestration and its efficiency optimization. *J. Chin. Urban For.* (04), 01–05.
- Wang, Y. N., Chang, Q., and Li, X. Y. (2021). Promoting sustainable carbon sequestration of plants in urban greenspace by planting design: a case study in parks of Beijing. *Urban For. & Urban Green.* 64, 127291. doi:10.1016/j.ufug.2021.127291
- Wang, J. N., Qin, N. X., and Jiang, T. (2022). Interpretation of IPCC AR6: impacts and adaptations of climate change on cities, settlements and key infrastructure. *Clim. Change Res.* 18 (4), 433–441. doi:10.14085/j.fjyl.2022.05.0017.07
- Wei, S. Y., Chen, Q. J., Wu, W. B., and Ma, J. (2021). Quantifying the indirect effects of urbanization on urban vegetation carbon uptake in the megacity of Shanghai, China. *Environ. Reserch Lett.* 16, 064088. doi:10.1088/1748-9326/ac06fd
- Wen, D. Z. (1997). Biomass study of the community of *Castanopsis chinensis*+*Cryptocarya a cininna*+*Schima superba* in a southern China reserve. *Acta Ecol. Sin.* (05), 497–504.
- Xue, C. Y., Wang, Z., and Cui, X. (2014). Carbon storage of poplar plantations in upper and middle reaches of Huangpu River, Shanghai. *Guihaia* 34 (3), 338–343.
- Yang, Y. F., Yu, C. H., Li, S., and David, B. (2024). A planting optimization strategy to improve the carbon sink benefit for urban green-Taking the communal green of Nanjing Forestry University as an example. *Ecol. Indic.* 159, 111619. doi:10.1016/j.ecolind.2024.111619
- Yao, Z. Y., Liu, J. J., Zhao, X. W., Dong, F. L., and Wang, L. (2015). Spatial dynamics of aboveground carbon stock in urban green space: a case study of Xi'an, China. *J. Arid Land* 7 (3), 350–360. doi:10.1007/s40333-014-0082-9
- Yi, L., and Wang, H. C. (2019). Discussion on calculation and optimization of benefits of carbon sequestration of plant communities in urban parks. *Landscape Design* (03), 36–43.
- Zhang, Y. (2019). *Quantitative assessment and optimization of carbon sequestration benefits of plant communities in construction waste landfill parks*. Thesis. Tianjin University.
- Zhang, C., Tian, H., Pan, S., Lockaby, G., and Chappelka, A. (2014). Multi-factor controls on terrestrial carbon dynamics in urbanized areas. *Biogeosciences* 11, 7107–7124. doi:10.5194/bg-11-7107-2014
- Zhang, X. J., Leng, H. B., Zhao, G. Q., Jun, J., Tu, A. C., Song, K., et al. (2018). Allometric models for estimating aboveground biomass for four common greening tree species in Shanghai City, China. *J. Nanjing For. Univ.* 42 (02), 141–146.
- Zhang, X. G., Huang, H. S., Tu, K., Li, R., Zhang, X. Y., Liu, Y., et al. (2024). Effects of plant community structural characteristics on carbon sequestration in urban green spaces. *Eff. plant community Struct. Charact. carbon sequestration urban green spaces. Sci. Rep.* 14 (14), 7382. doi:10.1038/s41598-024-57789-2
- Zhao, J., Chen, S., Jiang, B., Ren, Y., Wang, H., Vause, J., et al. (2013). Temporal trend of green space coverage in China and its relationship with urbanization over the last two decades. *Sci. Total Environ.* 442, 455–465. doi:10.1016/j.scitotenv.2012.10.014
- Zhao, X., Liu, J. J., and Bu, Y. K. (2021). Quantitative analysis of spatial heterogeneity and driving forces of the thermal environment in urban built-up areas: a case study in Xi'an, China. *Sustainability* 13 (4), 1870. doi:10.3390/su13041870
- Zhao, D., Cai, J., Xu, Y. M., Liu, Y. H., and Yao, M. M. (2023). Carbon sinks urban public green spaces under carbon neutrality a systematic literature review. *Urban For. Urban Green.* 86, 128037. doi:10.1016/j.ufug.2023.128037
- Zhu, M. (2020). *Study on the carbon fixation evaluate of the green-land system in the Xi'an ChanBa eco-region*. PhD Thesis. Xi'an University of Architecture and Technology.